

Article

# In Vitro Cytotoxicity and Antioxidant Studies of *Dovyallis caffra*-Mediated Cassiterite (SnO<sub>2</sub>) Nanoparticles

Jerry O. Adeyemi 

Postharvest and Agro-Processing Research Centre, Department of Botany and Plant Biotechnology, University of Johannesburg, Auckland Park, P.O. Box 524, Johannesburg 2006, South Africa; jerryadeyemi1st@gmail.com or oadeyemi@uj.ac.za; Tel.: +27-(071)-901-0236

**Abstract:** Many medicinal plants found in Africa, such as *Dovyallis caffra*, have been reported to contain various bioactive compounds, which have been found to reduce metal salts into their corresponding metal-based nanoparticles. In this paper, the evaluation of synthesis, characterization, and biological properties of *Dovyallis caffra*-mediated cassiterite (SnO<sub>2</sub>) nanoparticles was carried out. The physicochemical properties of the synthesized material were investigated using X-ray diffraction (XRD), energy dispersive X-ray analysis (EDX), scanning electron microscopy (SEM), and transmission electron microscopy (TEM) techniques. The characterization studies revealed that the material possessed a single tetragonal cassiterite SnO<sub>2</sub> phase, having a cluster-like foam appearance and an irregular spherical morphology with diameters ranging from 6.57 to 34.03 nm. The biological screening revealed that the prepared cassiterite (SnO<sub>2</sub>) nanoparticles exhibited cytotoxicity against the MCF-7 breast cancer cells, with an IC<sub>50</sub> value of 62.33 µg mL<sup>-1</sup>, better than the standard drug 5-fluorouracil, with an IC<sub>50</sub> value of 71.21 µg mL<sup>-1</sup>. The radical scavenging potential of the nanoparticles, using the DPPH assay, showed that it possessed a slightly better activity than ascorbic acid, a common antioxidant. These results suggest that the *Dovyallis caffra*-mediated cassiterite (SnO<sub>2</sub>) nanoparticles possess the potential to simultaneously generate and scavenge excess ROS, which in turn results in the exhibition of good cytotoxicity and antioxidant properties.

**Keywords:** cassiterite (SnO<sub>2</sub>); medicinal plant; nanoparticles; *Dovyallis caffra*; cytotoxicity; radical-scavenging properties



**Citation:** Adeyemi, J.O. In Vitro Cytotoxicity and Antioxidant Studies of *Dovyallis caffra*-Mediated Cassiterite (SnO<sub>2</sub>) Nanoparticles. *Sci. Pharm.* **2023**, *91*, 34. <https://doi.org/10.3390/scipharm91030034>

Academic Editor: Murali Mohan Yallapu

Received: 15 May 2023

Revised: 21 June 2023

Accepted: 30 June 2023

Published: 7 July 2023



**Copyright:** © 2023 by the author. Licensee MDPI, Basel, Switzerland. This article is an open access article distributed under the terms and conditions of the Creative Commons Attribution (CC BY) license (<https://creativecommons.org/licenses/by/4.0/>).

## 1. Introduction

Medicinal plants have been used in Africa for centuries in traditional medicine to treat various diseases [1]. These plants contain different bioactive compounds, such as alkaloids, flavonoids, terpenoids, and phenolic compounds, which have been found to have therapeutic properties [1]. One such plant, indigenous to many countries in Southern Africa, is *Dovyallis caffra*, commonly called Kei apple. *Dovyallis caffra* is a small tree or shrub native to the Kei River area of southwestern Africa (hence, the name). It is grown abundantly in the eastern regions of South Africa [1,2]. The fruits are nearly round bright yellow with tough skin, which is highly acidic, and an apricot-textured flesh [3]. The leaves are glossy, leathery, and oval to oblong, with serrated edges, typically arranged in an alternate pattern along the stem. The leaves are dark green and grow up to 10 cm long, with a characteristic aroma. Studies investigating the phytochemical composition of Kei apple leaves have identified various bioactive compounds, including flavonoids, tannins, alkaloids, and terpenoids, which are responsible for the medicinal properties and documented to possess antioxidant, antibacterial, antifungal, and anti-inflammatory activities [1].

The study of nanoparticles has gained significant attention in recent years due to their potential applications in various fields, including medicine. Multiple methods of synthesizing nanoparticles (NPs) have been explored, including chemical and physical

approaches, but there has been a growing interest in using medicinal plants for their synthesis [4]. The use of medicinal plants in the synthesis of nanoparticles has several advantages over traditional methods [5]. Firstly, it is a green synthesis method that does not require toxic chemicals, which may harm the environment and human health [5]. Secondly, the bioactive compounds present in medicinal plants can act as reducing agents, stabilizers, and capping agents, which can produce nanoparticles with desirable properties, such as uniform size distribution, high stability, and biocompatibility [6]. Thirdly, medicinal plants are readily available, cost-effective, and can be easily scaled up for large-scale production of nanoparticles [4].

Generally, the nanotechnology-based development of novel drug delivery systems is on the rise, with a specific interest in using metal-based nanoparticles [7]. Metal-based nanoparticles are thus gaining attention for their potential use as drug delivery systems and active agents in cancer therapy [8]. For instance, some reports have shown that metal oxide nanoparticles can selectively kill cancer cells without much affecting normal cells by exploiting ROS generation and oxidative stress conditions in tumour cells [7,9]. It was found that altering various physicochemical properties of some nanoparticles created a fine-tuned oxidative response in the cancer cells, which generated intracellular ROS levels to destroy the cancer cells without affecting normal cells. This emerging technology has the potential to revolutionize cancer therapy [7]. Among the various types of metal-based nanoparticles, tin (IV) oxide (SnO<sub>2</sub>) nanoparticles are generating serious interest due to their exceptional physicochemical properties, biocompatibility, and biological properties. Several studies have already investigated the influence of medicinal plants on the synthesis of SnO<sub>2</sub> nanoparticles. For instance, *Tradescantia spathacea* leaf extract was used to synthesize SnO<sub>2</sub> nanoparticles, exhibiting enhanced photo-antioxidant activities under visible light irradiation. This study highlights the potential of green synthesis methods for producing cost-effective SnO<sub>2</sub> NPs with photo-antioxidant activity [10]. Similarly, alongside other oxides, SnO<sub>2</sub> NPs with a crystallite size of about 5.23 nm have been synthesized using *Murraya koenigii* leaf extract [11]. Furthermore, undoped and cobalt doped SnO<sub>2</sub> NPs have been synthesized using *Clerodendrum inerme* aqueous extract, which showed great antibacterial and antifungal activities against *E. coli*, *B. subtilis*, *A. niger*, *A. flavus*, and *C. albicans* [12]. Moreover, upon the cytotoxicity screening, significant in vitro anticancer and in vivo antitumoral activities against the cancer cells and Ehrlich ascites tumour cell lines were reported, respectively, compared with the used standard. Hence, considering the already demonstrated useful biological properties of the SnO<sub>2</sub> NPs, I herein report the synthesis and the studies of physicochemical characteristics of *Dovyalis caffra*-mediated SnO<sub>2</sub> nanoparticles. Using both MTT and DPPH assay, the cytotoxic potentials against breast carcinoma cells (MCF-7) and the radical scavenging properties were evaluated.

## 2. Materials and Methods

### 2.1. Plant Preparation and Synthesis of SnO<sub>2</sub> Nanoparticles, Using Leaf Extracts of *Dovyalis c.*

*Dovyalis caffra* leaves were collected from the tree stalks at the North-West University Garden in Mafikeng. To remove any unwanted materials, the leaves were thoroughly washed with distilled water. They were then ground into a fine powder after being dried in the lab for 21 days in the open lab. About 1000 mL of deionized water and approximately 100 g of the obtained powder were heated for two hours at a temperature of 70 °C. The final extract was filtered using Whatman filter paper with a retention pore size of 11 m. The SnO<sub>2</sub> nanoparticles were prepared using the procedure described in the literature [5]. A few drops of NaOH solution were added to 50 mL of the extract to keep the solution alkaline, followed by the addition of about 160 mL of 1 mM stannous chloride (SnCl<sub>2</sub>). The resulting mixture was then stirred at 80 °C for an hour. The following colour changes from orange-yellow to white indicated the formation of the nanoparticles. After the reaction was adjudged completed, the resulting mixture was washed with deionized water and ethanol to collect the particles, centrifuged at 10,000 rpm for 15 min, dried in an oven for 12 h, and then calcined at 400 °C for 2 h in a muffle furnace.

## 2.2. Characterization of SnO<sub>2</sub> Nanoparticles

The crystalline phase of the SnO<sub>2</sub> nanoparticles was examined using the Rontgen PW3040/60 X'Pert Pro XRD diffractometer, (Almelo, Netherlands), which is outfitted with nickel-filtered Cu K radiation ( $k = 1.5418$ ) at room temperature and has a scanning rate of  $0.0018^\circ \text{ min}^{-1}$ . To describe the morphological features of the materials, TECNAI G2 (ACI) scanning and transmission electron microscopy with an accelerating voltage of 200 kV were employed. The material's elemental makeup and surface morphology were investigated using the FEI Quanta FEG 250 field emission gun microscope operating at 15 kV. Using the Oxford Inca software, the energy dispersive X-ray (EDX) spectra were collected.

## 2.3. Cytotoxicity Study Using MTT Assay

According to a similar procedure [13], the in vitro cytotoxicity study using MCF7 breast cancer cell lines procured from ATCC, Manassas, USA, was carried out. The cells were grown in EMEM, which included 10% foetal bovine serum, 100 g/mL penicillin, and 100 g/mL streptomycin in 25 cm<sup>2</sup> tissue culture flasks. The vitality of the MCF7 cells was examined using the MTT test in a 96-well plate with  $2.5 \times 10^2$  cells/well in 100 L EMEM cells. The produced cells were then cultured at 37 °C for an overnight period. The medium was changed, and samples were added at different concentrations (20, 40, 80, and 100 g/mL). The MTT assay was performed after the cells had been cultured for 48 h at 37 °C. 5-Fluorouracil was employed as the standard, while untreated cells were used as positive control 1 and untreated cells with DMSO as positive control 2. The media in the experiment was changed to a fresh medium containing 10% MTT reagent, and then it was incubated at 37 °C for 4 h. This was taken out, the insoluble formazan crystals were dissolved in 100 L of DMSO, and then absorbance values at 570 nm were taken using DMSO as a control. This procedure was repeated thrice.

## 2.4. Antioxidant Potential Study of SnO<sub>2</sub> NPs, Using DPPH Assay

The ability of the SnO<sub>2</sub> NPs to scavenge 2,2-diphenyl-1-picrylhydrazyl hydrate (DPPH) free radicals was evaluated using an established published procedure [13]. A total of 100 mL of methanol was used to prepare the DPPH stock solution, which was left in the dark for 30 min. The nanoparticles were prepared as a 50 mg/mL stock solution in methanol and then serially diluted to make 25, 12.5, 6.25, and 3.12 mg/mL. Using a microplate reader, model 680-BIO-RAD (Bio-Rad, Hercules, CA, USA), 250 µL of the DPPH mixture was pipetted into a 96-well microplate in triplicates, and absorbance was measured at 515 nm and compared to the control containing 1 mL of methanol. Within the same concentration range, ascorbic acid was used as a standard drug to compare the material's efficacy as a good scavenging agent. Then, equation 1 was employed to estimate the percentage of scavenging activity of the material:

$$\% \text{ scavenging} = \frac{Ab_c - Ab_s}{Ab_c} \times 100 \quad (1)$$

$Ab_c$  is the absorbance of the control (contains all reagents except the SnO<sub>2</sub> NPs), while  $Ab_s$  is the absorbance of SnO<sub>2</sub> (contains all reagents including the SnO<sub>2</sub> NPs).

## 3. Results and Discussions

### 3.1. Synthesis

The different phytochemicals present in plants play a significant role in the synthesis and the resulting physicochemical properties of the synthesized nanoparticles [14]. *Dovyalis caffra*, as already stated, contains several of these bioactive compounds, including flavonoids, phenolic acids, lignans, and stilbenes [15]. Amongst these groups, flavonoids have been mostly implicated in playing a significant role in synthesizing various nanoparticles in the literature [16]. They have been reported to act as both reducing and stabilizing agents in forming the SnO<sub>2</sub> nanoparticles in a three-step process (see Figure 1a) [2,17]. These steps involve (i) the reduction of Sn<sup>2+</sup> to Sn<sup>0</sup>, (ii) the reducing effect of polyphenols

on  $\text{Sn}^0$  species, and (iii) the phase transformation of  $\text{Sn}^0$  species into the  $\text{SnO}_2$  nanoparticles at higher temperatures. Catechin, an example of a flavonoid already identified in the plants [2,17], is polar (water-soluble) and serves as both a stabilizing and capping agent during the reaction [16]. The lone pairs of electrons in the polar groups of catechin occupy  $2sp$  orbitals of an  $\text{Sn}^{2+}$  ion to form an  $\text{Sn}^{2+}$  complex, which reduces  $\text{Sn}^{2+}$  to  $\text{Sn}^0$ . The reduction of  $\text{Sn}^{2+}$  capped with phenolic compounds forms small  $\text{Sn}^0$  nanoparticles inside the nanoscopic templates that are then transformed into the  $\text{SnO}_2$  nanoparticles upon air annealing [16]. A summary of the synthetic procedure of the *Dovyalis caffra*-mediated cassiterite ( $\text{SnO}_2$ ) nanoparticles is presented in Figure 1b.

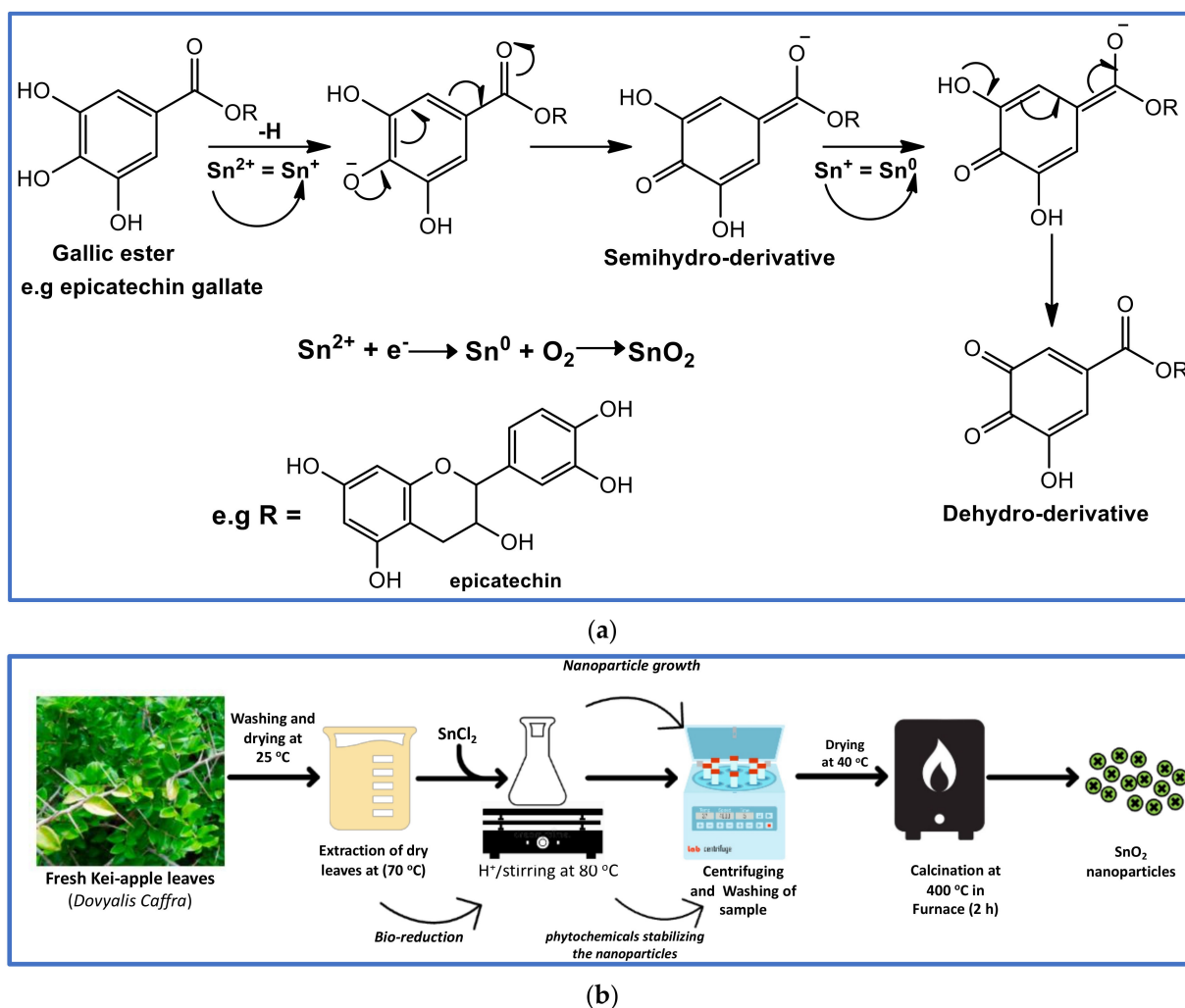


**Figure 1.** (a) Probable reaction mechanism involved in preparing *Dovyallis caffra*-mediated cassiterite ( $\text{SnO}_2$ ) nanoparticles. Adapted from [16], (b) pictorial representation of the synthetic pathway of *Dovyallis caffra*-mediated  $\text{SnO}_2$  nanoparticles.

### 3.2. XRD Analysis Study of $\text{SnO}_2$ NPs

The X-ray diffraction analysis of the prepared  $\text{SnO}_2$  NPs was carried out to determine the phase and crystal structure and estimate the average size. Hence, the diffractogram measured in the  $2\theta$  range of  $20\text{--}80^\circ$  was collected and is presented in Figure 2. The observed XRD peaks at  $2\theta$  and their corresponding lattice indices are shown in Table 1. The estimated value of lattice constant from different ( $hkl$ ) planes was determined by using the formula  $a = d\sqrt{h^2 + k^2 + l^2}$ , where  $d$  is the inter-planer distance, and ( $hkl$ ) are Miller indices. Furthermore, the estimated values of the lattice constant were  $a = 4.73820 \text{ \AA}$  and  $c = 3.18710 \text{ \AA}$ . The diffracted pattern observed thus indicates that the material prepared

possessed a tetragonal structure that conforms to the tin oxide (SnO<sub>2</sub>) cassiterite polycrystalline phase with JCPDS card No. 00-041-1445. No other crystalline peaks were found in the pattern, which indicates that the material had a pure structure. From the obtained diffractogram, the average crystallite size (D), using Scherrer equation, was estimated to be 10.11 nm, as seen in Table 1. Other reports involving the use of other plant extracts have also assessed the crystallite size (D), using Scherrer equation. For instance, Suresh et al., using *Delonix elata* leaf extract, found the crystallite size of the SnO<sub>2</sub> nanoparticles to be 7.61, 6.09, and 5.92 nm, using sonication, wet chemical, and microwave methods [18]. Similarly, Fatimah et al. also found the crystallite size to be 18.2 nm, using fresh *Pometia pinnate* leaves [19].

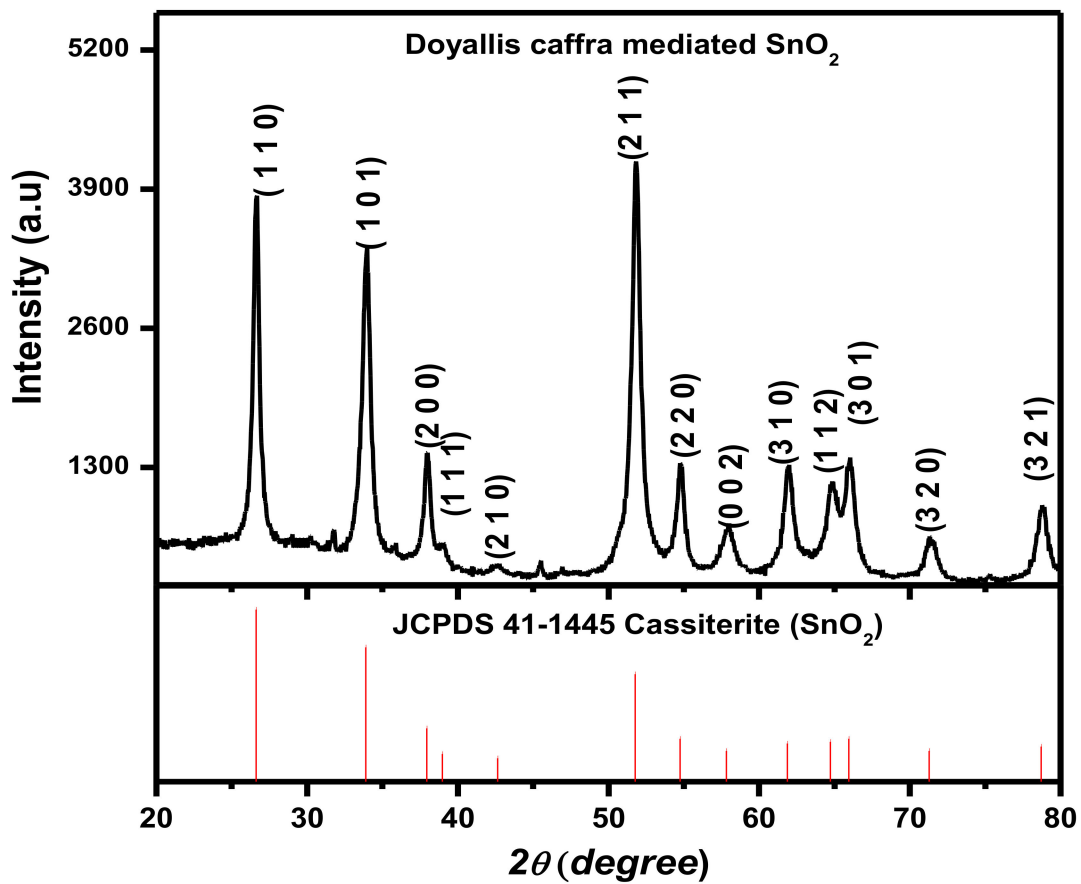


Figure 2. The obtained XRD pattern for prepared SnO<sub>2</sub> (cassiterite) nanoparticles.

Table 1. The estimated data collected from the crystallite size (D) calculations showing the miller indices and their corresponding 2θ angles.

S/No	Peaks (2θ)	hkl	FWHM	Crystallite Size (D) nm	D (Average) nm
1	26.11	110	0.63	12.35	10.11
2	33.89	101	0.77	9.29	
3	37.95	200	0.54	13.88	
4	38.96	111	0.58	12.99	
5	42.64	210	7.73	0.96	
6	51.78	211	0.77	9.28	
7	54.76	220	0.56	12.51	
8	57.82	002	0.58	11.98	

Table 1. Cont.

S/No	Peaks (2 $\theta$ )	<i>hkl</i>	FWHM	Crystallite Size (D) nm	D (Average) nm
9	61.87	310	0.66	10.30	
10	64.72	112	0.89	7.49	
11	65.94	301	0.69	9.58	
12	71.28	202	0.41	15.67	
13	78.71	321	0.56	10.97	

### 3.3. Microscopic Analysis

The morphologies of the prepared material were studied using SEM at higher magnification and TEM at lower magnification, as shown in Figure 3A,B. The SEM images revealed that the prepared SnO<sub>2</sub> forms a cluster-like foam with agglomeration, as seen in Figure 3A, similar to the findings of a report in the literature [18]. Furthermore, the TEM analysis distinctively showed the irregular spherical morphology for the prepared SnO<sub>2</sub> nanoparticles. The diameter sizes found for the material, using ImageJ, the origin software, and the histogram distribution curve presented in Figure 3C (inset), were between 6.57 and 34.03 nm. The average diameter size was estimated to be 15.57 nm, within the range found for the estimated crystallite size (D), 10.11 nm. Other reports using *Camellia sinensis* flower extract [16], *Red spinach* leaf extract [20], *Galaxaura elongate* [21], and *Vitex altissima* (L.) leaf extract [22] described similar spherical morphologies with diameter sizes of 5–30, 20–40, 35, and 20 nm, respectively. The collected EDS spectra shown in Figure 3C indicate that the elemental constituent found in the material consists only of Sn and O. However, the appearance of a carbon peak is attributed to the tape used to support the nanoparticles in the sample holder, as reported in other studies [5].

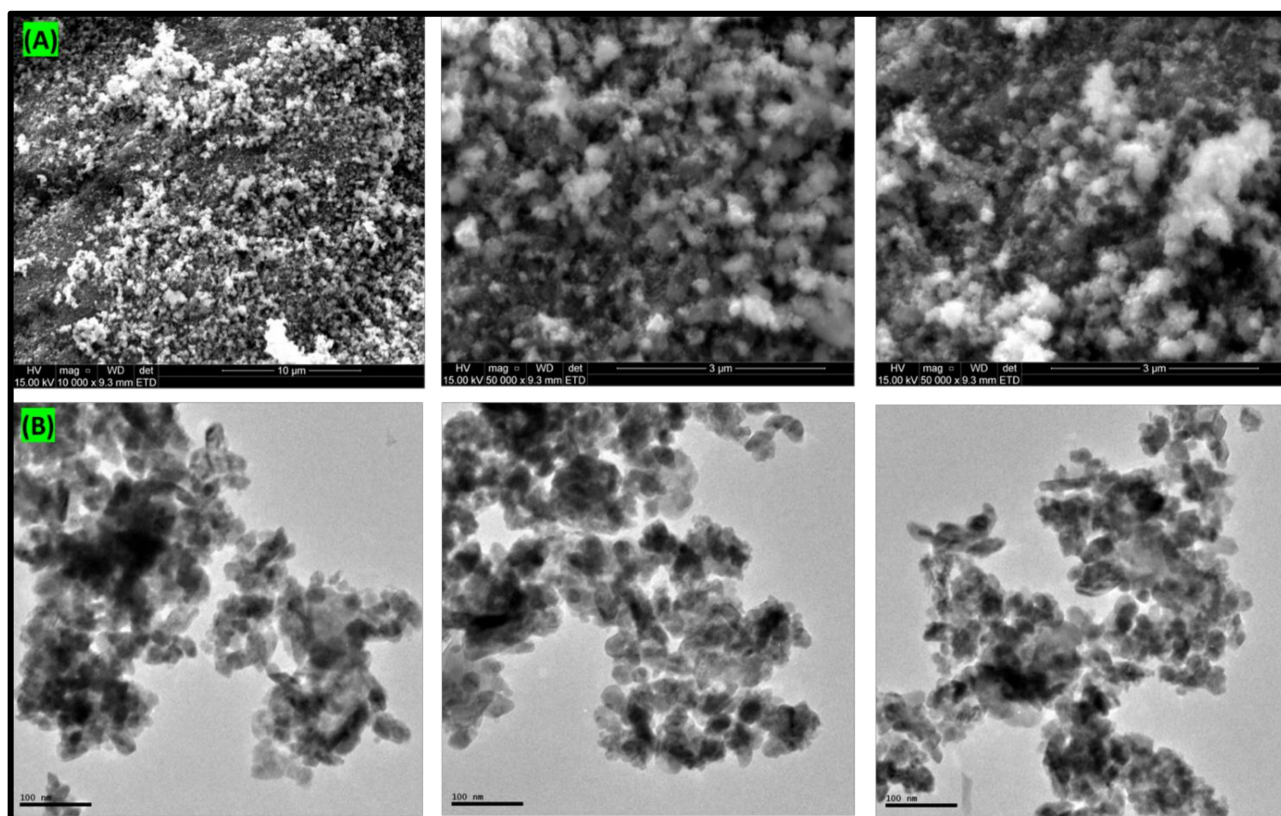
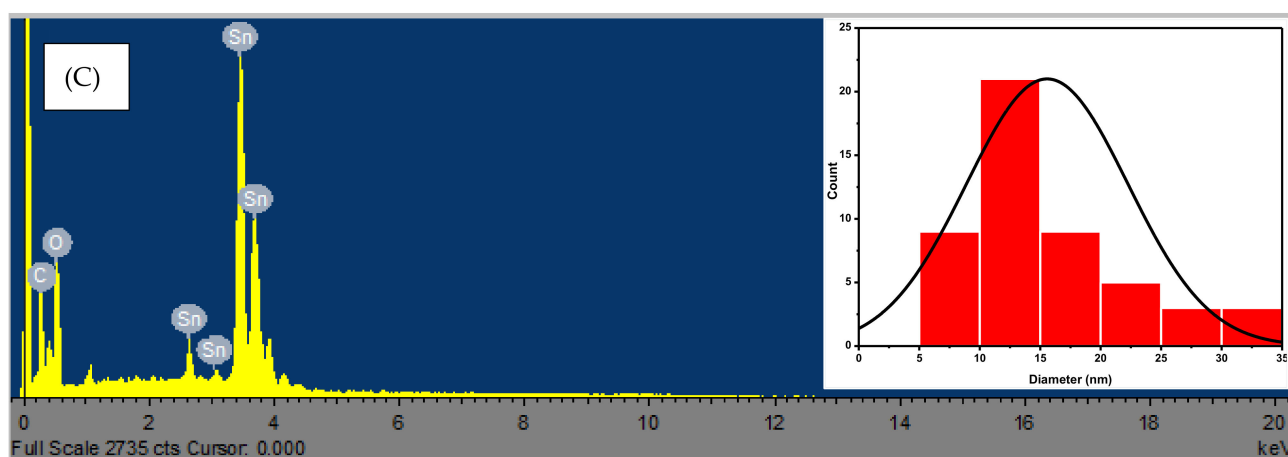


Figure 3. Cont.



**Figure 3.** Micrographs of (A) SEM and (B) TEM images at different magnifications were collected for the prepared SnO<sub>2</sub> nanoparticles. (C) The EDS spectra of the prepared SnO<sub>2</sub> nanoparticles (inset: histogram distribution diagram for particle sizes).

### 3.4. Cytotoxicity of SnO<sub>2</sub> Nanoparticles

The cytotoxic effect of the SnO<sub>2</sub> nanoparticles in the human breast cancer (MCF-7) cell line was evaluated using the MTT assay approach. The obtained data from this study are presented in Table 2 below, alongside the estimated minimum inhibitory concentration (IC<sub>50</sub>). These results showed a concentration-dependent profile, in which the cell viability reduces as the concentration of the SnO<sub>2</sub> nanoparticles increases. The results were compared to a standard anticancer drug, 5-fluorouracil (5-FUC). Generally, the prepared material was more potent at lower concentrations than the standard drug. For instance, at the smallest concentration of 20 µg mL<sup>-1</sup>, about 73% of the cells survived, whereas in 5-FUC, about 98% of the cells were viable at the same concentration. However, there was a change at over 60 µg mL<sup>-1</sup>; the performance of the standard drug in killing the cells was better than that of the SnO<sub>2</sub> nanoparticles, as about 37% of the cells were viable at the used highest concentration compared to the 57% viability for the SnO<sub>2</sub> nanoparticles. Nevertheless, the estimated IC<sub>50</sub> values of the SnO<sub>2</sub> nanoparticles and 5-FUC were 62.33 and 71.21 µg mL<sup>-1</sup>, respectively, indicating that the prepared material is slightly more cytotoxic than the 5-FUC. Other studies have reported the cytotoxicity of SnO<sub>2</sub> nanoparticles in the literature, but none of them has prepared this material using the Kei-apple plant leaf extracts. For instance, using a sol-gel preparatory approach, Ahamed et al. found that SnO<sub>2</sub> nanoparticles induced cytotoxicity, cell cycle arrest, and low mitochondrial membrane potential in a dose- and time-dependent manner [7]. This study highlighted that the prepared SnO<sub>2</sub> nanoparticles can potentially kill cancer cells via the oxidative stress pathway. Tammina et al. also reported the cytotoxicity effect of different-size tetragonal tin oxide nanoparticles (SnO<sub>2</sub> NPs) synthesized using *Piper nigrum* seed extract against the colorectal (HCT116) and lung (A549) cancer cell lines and found that the proliferation of both cell lines increased with the decreasing nanoparticles' size [23]. From the literature, the most probable pathway for the cytotoxicity mechanism of the prepared SnO<sub>2</sub> nanoparticles is thus presented in Figure 4 [24].

**Table 2.** Cell viability activities in percentages at different concentrations (µg mL<sup>-1</sup>) of SnO<sub>2</sub> and 5-FUC.

Samples (µg mL <sup>-1</sup> )	Control (Cells Only)	Control (Cells + DMSO)	100	80	40	20	IC <sub>50</sub>
SnO <sub>2</sub> (%)	100.00	100.59	57.26	60.43	70.91	73.72	62.33
5-FUC (%)	100.00	100.59	37.23	53.81	73.06	98.44	71.21

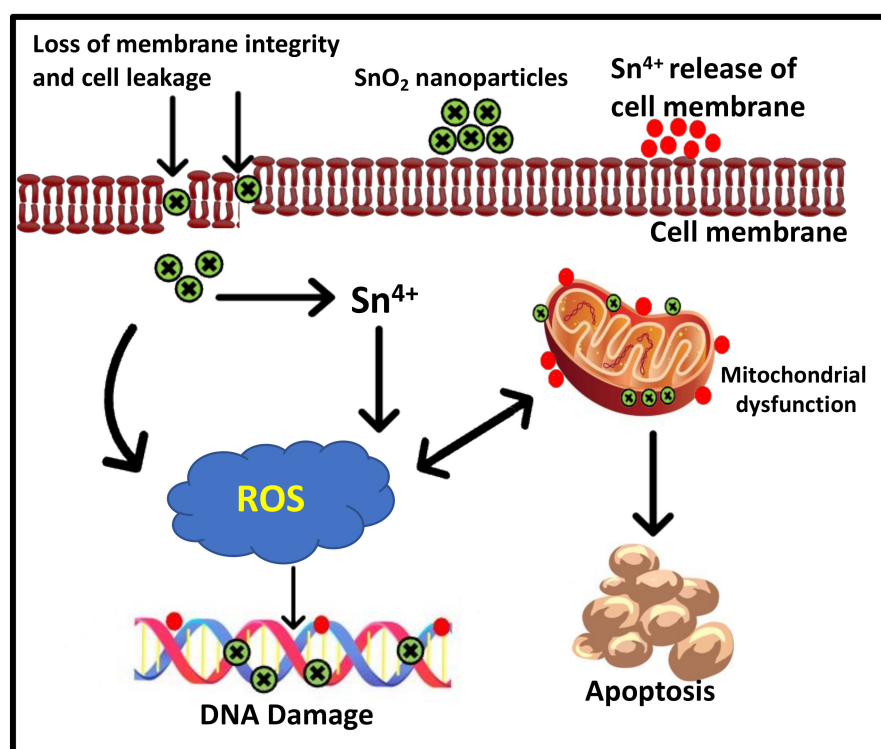


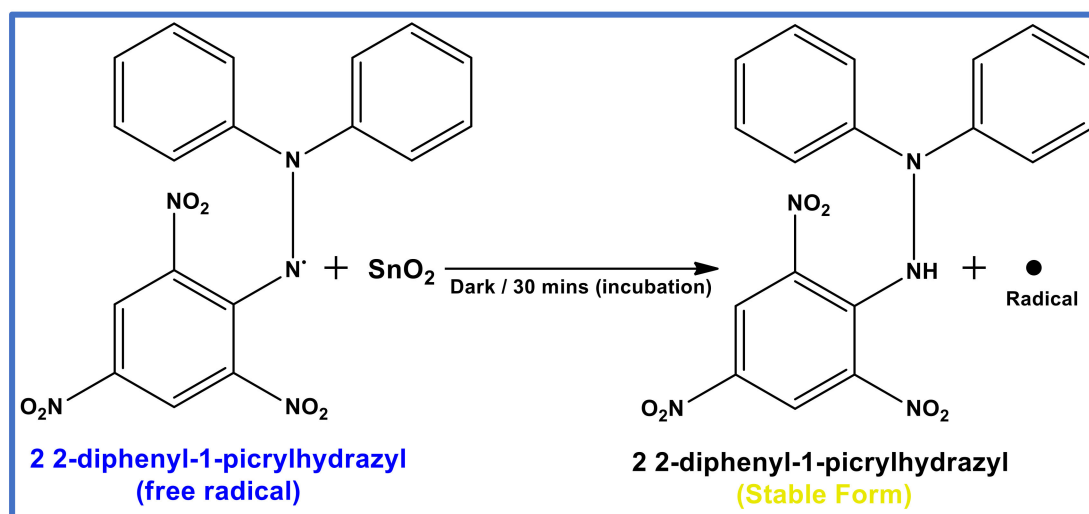
**Figure 4.** Probable pathway mechanism of cytotoxicity effect of  $\text{SnO}_2$  (adapted with permission from [24] Springer, 2023).

### 3.5. Free Radical Scavenging Potential of $\text{SnO}_2$ Nanoparticles, Using DPPH Assay

Many free radicals are generated in humans due to several biomolecular interactions involving molecular oxygen. Hence, the need to remove excessive and unwanted radicals that may harm the body [25]. Several studies have thus been carried out to evaluate the potential of several compounds and materials, including nanoparticles, as ameliorating agents [25]. Different approaches and assays have been employed to determine the scavenging properties of both natural and synthetic compounds. Still, the most recognized approach is using 2,2-diphenyl-1-picrylhydrazyl hydrate (DPPH), a standard nitrogen-concentrated free radical that measures the intensive scavenger function of many compounds [13]. In this free radical scavenging method, the relaxation of DPPH is brought about by hydrogen or electron transfer acceptance, reducing its intensity [13]. This approach was employed in this study, and the data obtained are presented in Table 3 and compared with a known antioxidant agent (ascorbic acid). A dose-dependent pattern was observed as the concentration increased from 3.13 to 50  $\text{mg mL}^{-1}$ . At the used lowest concentration, about 23% of reactive oxygen species were scavenged by the  $\text{SnO}_2$  nanoparticles compared to the 4% by ascorbic acid. At the highest concentration, however, more than 50% of the radicals were scavenged by ascorbic acid compared to about 47% by the prepared  $\text{SnO}_2$  nanoparticles, which implies that the material compares favourably with ascorbic acid. Furthermore, the estimated  $\text{IC}_{50}$  showed that the prepared  $\text{SnO}_2$  nanoparticles are slightly better than the known drug used in this study. The mechanism of action is thought to follow a similar pathway as that of other metal oxide nanoparticles reported in the literature [26]. The observed activity was attributed to the small size of the nanoparticles and also the transfer of electron density from the oxygen atom to the odd electron located on the nitrogen atom in DPPH (see Figure 5), resulting in the decrease of  $n \rightarrow \pi$  transition intensity, which gives off a strong absorption maximum at 515 nm [27]. This resulted in the colour change from the blue unstable methanolic DPPH solution to yellow upon adding  $\text{SnO}_2$ , as seen in Figure 5. This study thus further strengthens the already existing assertion of the potential of metal-based nanoparticles as good antioxidants.

**Table 3.** Radical scavenging activities in percentages at different concentrations ( $\text{mg mL}^{-1}$ ) of  $\text{SnO}_2$  and ascorbic acid.

Samples ( $\text{mg mL}^{-1}$ )	3.13	6.3	12.5	25	50	$\text{IC}_{50}$
$\text{SnO}_2$ (%)	23.32	28.59	33.52	42.71	46.98	4.68
Ascorbic acid (%)	4.08	12.63	34.88	39.25	52.75	4.95



promoting cancer cell death. At the same time, their free radical scavenging properties can help to mitigate potential damage to healthy cells and maintain overall redox balance.

It is worth noting that the specific mechanisms underlying these functions and their precise balance may vary depending on the physicochemical characteristics of the SnO<sub>2</sub> nanoparticles, such as size, surface properties, and functionalization. Nevertheless, further research is necessary to fully understand the intricate relationship between oxidative stress induction and free radical scavenging by the SnO<sub>2</sub> nanoparticles and to optimize their therapeutic applications.

#### 4. Conclusions

This study, for the first time, reports the synthesis of *Dovyalis caffra*-mediated SnO<sub>2</sub> nanoparticles. The single tetragonal phase of the cassiterite SnO<sub>2</sub> nanoparticles was confirmed using the XRD analysis and used to estimate the crystallite size (D), found to be 10.11 nm. Other physicochemical properties, using the SEM techniques, showed that this material possessed a cluster-like foam morphology with agglomeration, while the TEM analysis revealed that this material had a distinctively irregular spherical morphology, with diameters ranging between 6.57 and 34.03 nm. Hence, the average diameter found was estimated to be 15.57 nm, which agrees with the estimated crystallite size (D). Furthermore, this cytotoxicity study showed that the SnO<sub>2</sub> nanoparticles (IC<sub>50</sub> = 62.33 µg mL<sup>-1</sup>) possessed better cytotoxicity than the standard 5-fluorouracil (IC<sub>50</sub> = 71.21 µg mL<sup>-1</sup>) upon screening against the MCF-7 breast cancer cells. Similarly, the radical scavenging potential of the SnO<sub>2</sub> nanoparticles, using a DPPH assay, showed that they (IC<sub>50</sub> = 4.68 mg mL<sup>-1</sup>) possessed a slightly better activity than ascorbic acid, a known antioxidant drug (IC<sub>50</sub> = 4.95 mg mL<sup>-1</sup>). The biological results here thus indicate the potentials of the *Dovyalis caffra*-mediated SnO<sub>2</sub> nanoparticles (synthesized in a facile eco-friendly route) to effectively generate and simultaneously scavenge excess ROS, which induces oxidative stress in the cancer cells and prevent their accumulation, respectively.

**Author Contributions:** J.O.A.: conceptualization, methodology, writing, editing, and review of the original draft paper. The author has read and agreed to the published version of the manuscript.

**Funding:** This research received no external funding.

**Institutional Review Board Statement:** Not applicable.

**Data Availability Statement:** Not applicable.

**Acknowledgments:** The author acknowledges the contribution of the University of Johannesburg for the financial support towards his research fellowship. Likewise, the author acknowledges the support of M. Singh from the University of KwaZulu-Natal for her contribution to this cytotoxicity study. Furthermore, the author recognizes the supervision and guidance of Olaniyi Fawole from the University of Johannesburg.

**Conflicts of Interest:** The author declares no conflict of interest.

#### References

1. Aremu, A.O.; Ncama, K.; Omotayo, A.O. Ethnobotanical Uses, Biological Activities and Chemical Properties of Kei-Apple [*Dovyalis caffra* (Hook.f. & Harv.) Sim]: An Indigenous Fruit Tree of Southern Africa. *J. Ethnopharmacol.* **2019**, *241*, 111963. [[CrossRef](#)]
2. Loots, D.T.; Van Der Westhuizen, F.H.; Jerling, J. Polyphenol Composition and Antioxidant Activity of Kei-Apple (*Dovyalis caffra*) Juice. *J. Agric. Food Chem.* **2006**, *54*, 1271–1276. [[CrossRef](#)] [[PubMed](#)]
3. Taher, M.A.; Tadros, L.K.; Dawood, D.H. Phytochemical Constituents, Antioxidant Activity and Safety Evaluation of Kei-Apple Fruit (*Dovyalis caffra*). *Food Chem.* **2018**, *265*, 144–151. [[CrossRef](#)] [[PubMed](#)]
4. Adeyemi, J.O.; Oriola, A.O.; Onwudiwe, D.C.; Oyediji, A.O. Plant Extracts Mediated Metal-Based Nanoparticles: Synthesis and Biological Applications. *Biomolecules* **2022**, *12*, 627. [[CrossRef](#)]
5. Adeyemi, J.O.; Onwudiwe, D.C.; Oyediji, A.O. In Vitro  $\alpha$ -Glucosidase Enzyme Inhibition and Anti-Inflammatory Studies of Mn<sub>3</sub>O<sub>4</sub> Nanoparticles Mediated Using Extract of *Dalbergiella welwitschia*. *Results Chem.* **2022**, *4*, 100497. [[CrossRef](#)]
6. Adeyemi, J.O.; Elemike, E.E.; Onwudiwe, D.C. ZnO Nanoparticles Mediated by Aqueous Extracts of *Dovyalis caffra* Fruits and the Photocatalytic Evaluations. *Mater. Res. Express* **2019**, *6*, 125091. [[CrossRef](#)]

7. Ahamed, M.; Akhtar, M.J.; Majeed Khan, M.A.; Alhadlaq, H.A. Oxidative Stress Mediated Cytotoxicity of Tin (IV) Oxide (SnO<sub>2</sub>) Nanoparticles in Human Breast Cancer (MCF-7) Cells. *Colloids Surf. B Biointerfaces* **2018**, *172*, 152–160. [[CrossRef](#)]
8. Ramasamy, T.; Ruttala, H.B.; Sundaramoorthy, P.; Poudel, B.K.; Youn, Y.S.; Ku, S.K.; Choi, H.G.; Yong, C.S.; Kim, J.O. Multimodal Selenium Nanoshell-Capped Au@SiO<sub>2</sub> Nanoplatform for NIR-Responsive Chemo-Photothermal Therapy against Metastatic Breast Cancer. *NPG Asia Mater.* **2018**, *10*, 197–216. [[CrossRef](#)]
9. Ostrovsky, S.; Kazimirsky, G.; Gedanken, A.; Brodie, C. Selective Cytotoxic Effect of ZnO Nanoparticles on Glioma Cells. *Nano Res.* **2009**, *2*, 882–890. [[CrossRef](#)]
10. Matussin, S.N.; Harunsani, M.H.; Tan, A.L.; Mohammad, A.; Cho, M.H.; Khan, M.M. Photoantioxidant Studies of SnO<sub>2</sub> Nanoparticles Fabricated Using Aqueous Leaf Extract of *Tradescantia spathacea*. *Solid State Sci.* **2020**, *105*, 106279. [[CrossRef](#)]
11. Goel, A.; Tomar, S. Green Synthesis and Characterization of *Murraya koenigii* Leaf Extract Mediated IrO<sub>2</sub>, SnO<sub>2</sub>, and Ir-SnO<sub>2</sub> Nanoparticles. *Inorg. Nano-Met. Chem.* **2022**, 1–15. [[CrossRef](#)]
12. Khan, S.A.; Kanwal, S.; Rizwan, K.; Shahid, S. Enhanced Antimicrobial, Antioxidant, in Vivo Antitumor and in Vitro Anti-cancer Effects against Breast Cancer Cell Line by Green Synthesized Un-Doped SnO<sub>2</sub> and Co-Doped SnO<sub>2</sub> Nanoparticles from *Clerodendrum inerme*. *Microb Pathog.* **2018**, *125*, 366–384. [[CrossRef](#)] [[PubMed](#)]
13. Adeyemi, J.O.; Onwudiwe, D.C.; Oyedeji, A.O. Biogenic Synthesis of CuO, ZnO, and CuO–ZnO Nanoparticles Using Leaf Extracts of *Dovyalis caffra* and Their Biological Properties. *Molecules* **2022**, *27*, 3206. [[CrossRef](#)]
14. Adeyemi, J.O.; Elemike, E.E.; Onwudiwe, D.C.; Singh, M. Bio-Inspired Synthesis and Cytotoxic Evaluation of Silver-Gold Bimetallic Nanoparticles Using Kei-Apple (*Dovyalis caffra*) Fruits. *Inorg. Chem. Commun.* **2019**, *109*, 107569. [[CrossRef](#)]
15. Waweru, D.M.; Arimi, J.M.; Marete, E.; Jacquier, J.C.; Harbourne, N. Current Status of Utilization and Potential of *Dovyalis caffra* Fruit: Major Focus on Kenya—A Review. *Sci. Afr.* **2022**, *16*, e01097. [[CrossRef](#)]
16. Selvakumari, J.C.; Ahila, M.; Malligavathy, M.; Padiyan, D.P. Structural, Morphological, and Optical Properties of Tin(IV) Oxide Nanoparticles Synthesized Using *Camellia sinensis* Extract: A Green Approach. *Int. J. Miner. Metall.* **2017**, *24*, 1043–1051. [[CrossRef](#)]
17. Beer, T. Polyphenols, Ascorbate and Antioxidant Capacity of the Kei-Apple (*Dovyalis caffra*). Master's Thesis, Potchefstroom Campus of the North-West University, Potchefstroom, South Africa, 2006.
18. Suresh, K.C.; Surendhiran, S.; Manoj Kumar, P.; Ranjith Kumar, E.; Khadar, Y.A.S.; Balamurugan, A. Green Synthesis of SnO<sub>2</sub> Nanoparticles Using *Delonix elata* Leaf Extract: Evaluation of Its Structural, Optical, Morphological and Photocatalytic Properties. *SN Appl. Sci.* **2020**, *2*, 1735. [[CrossRef](#)]
19. Fatimah, I.; Purwiandono, G.; Hidayat, H.; Sagadevan, S.; Ghazali, S.A.I.S.M.; Oh, W.C.; Doong, R.A. Flower-like SnO<sub>2</sub> Nanoparticle Biofabrication Using *Pometia pinnata* Leaf Extract and Study on Its Photocatalytic and Antibacterial Activities. *Nanomaterials* **2021**, *11*, 3012. [[CrossRef](#)]
20. Wicaksono, W.P.; Sahroni, I.; Saba, A.K.; Rahman, R.; Fatimah, I. Biofabricated SnO<sub>2</sub> nanoparticles Using Red Spinach (*Amaranthus tricolor* L.) Extract and the Study on Photocatalytic and Electrochemical Sensing Activity. *Mater. Res. Express* **2020**, *7*, 7. [[CrossRef](#)]
21. Al-Enazi, N.M.; Ameen, F.; Alsamhary, K.; Dawoud, T.; Al-Khattaf, F.; AlNadhari, S. Tin Oxide Nanoparticles (SnO<sub>2</sub>-NPs) Synthesis Using *Galaxaura elongata* and Its Anti-Microbial and Cytotoxicity Study: A Greenery Approach. *Appl. Nanosci.* **2023**, *13*, 519–527. [[CrossRef](#)]
22. Bhosale, T.T.; Shinde, H.M.; Gavade, N.L.; Babar, S.B.; Gawade, V.V.; Sabale, S.R.; Kamble, R.J.; Shirke, B.S.; Garadkar, K.M. Biosynthesis of SnO<sub>2</sub> Nanoparticles by Aqueous Leaf Extract of *Calotropis gigantea* for Photocatalytic Applications. *J. Mater. Sci. Mater. Electron.* **2018**, *29*, 6826–6834. [[CrossRef](#)]
23. Tammina, S.K.; Mandal, B.K.; Ranjan, S.; Dasgupta, N. Cytotoxicity Study of *Piper nigrum* Seed Mediated Synthesized SnO<sub>2</sub> Nanoparticles towards Colorectal (HCT116) and Lung Cancer (A549) Cell Lines. *J. Photochem. Photobiol. B* **2017**, *166*, 158–168. [[CrossRef](#)]
24. Gebreslassie, Y.T.; Gebretnsae, H.G. Green and Cost—Effective Synthesis of Tin Oxide Nanoparticles: A Review on the Synthesis Methodologies, Mechanism of Formation, and Their Potential Applications. *Nanoscale Res. Lett.* **2021**, *16*, 97. [[CrossRef](#)] [[PubMed](#)]
25. Dobrucka, R. Antioxidant and Catalytic Activity of Biosynthesized CuO Nanoparticles Using Extract of *Galeopsis herba*. *J. Inorg. Organomet Polym. Mater.* **2018**, *28*, 812–819. [[CrossRef](#)]
26. Siripireddy, B.; Mandal, B.K. Facile Green Synthesis of Zinc Oxide Nanoparticles by *Eucalyptus globulus* and Their Photocatalytic and Antioxidant Activity. *Adv. Powder Technol.* **2017**, *28*, 785–797. [[CrossRef](#)]
27. Vidhu, V.K.; Philip, D. Phytosynthesis and Applications of Bioactive SnO<sub>2</sub> Nanoparticles. *Mater. Charact.* **2015**, *101*, 97–105. [[CrossRef](#)]
28. Liang, X.; Zhang, Q.; Wang, X.; Yuan, M.; Zhang, Y.; Xu, Z.; Li, G.; Liu, T. Reactive Oxygen Species Mediated Oxidative Stress Links Diabetes and Atrial Fibrillation. *Mol. Med. Rep.* **2018**, *17*, 4933–4940. [[CrossRef](#)]

**Disclaimer/Publisher's Note:** The statements, opinions and data contained in all publications are solely those of the individual author(s) and contributor(s) and not of MDPI and/or the editor(s). MDPI and/or the editor(s) disclaim responsibility for any injury to people or property resulting from any ideas, methods, instructions or products referred to in the content.